Calcium-Modulated Supervised Spike-Timing-Dependent Plasticity for Readout Training and Sparsification of the Liquid State Machine

Yingyezhe Jin and Peng Li
Department of Electrical and Computer Engineering
Texas A&M University, College Station, Texas, USA, 77840
Emails: {jyyz, pli}@tamu.edu

***Abstract*—The Liquid State Machine (LSM) is a promising model of recurrent spiking neural networks. It consists of a fixed recurrent network, or the reservoir, which projects to a readout layer through plastic readout synapses. The classification performance is highly dependent on the training of readout synapses which tend to be very dense and contribute significantly to the overall network complexity. We present a unifying biologically inspired calcium-modulated supervised spike-timing-dependent plasticity (STDP) approach to training and sparsification of readout synapses, where supervised temporal learning is modulated by the post-synaptic firing level characterized by the post-synaptic calcium concentration. The proposed approach prevents synaptic weight saturation, boosts learning performance, and sparsifies the connectivity between the reservoir and readout layer. Using the recognition rate of spoken English letters adopted from the TI46 speech corpus as a measure of performance, we demonstrate that the proposed approach outperforms a baseline supervised STDP mechanism by up to 25%, and a competitive non-STDP spike-dependent training algorithm by up to 2.7%. Furthermore, it can prune out up to 30% of readout synapses without causing significant performance degradation.**

I. INTRODUCTION

Reservoir computing, a biologically plausible computational paradigm that exploits complex recurrent spiking neural networks [1], has attracted a great deal of interest recently. The liquid state machine (LSM), one specific form of reservoir computing, has recently emerged in theoretical neuroscience [2]. As shown in Fig. 1, the LSM consists of a fixed "reservoir", a randomly connected recurrent spiking neural network (SNN) resembling biological cortical microcircuitry in the brain, and a layer of readout neurons that make classification decisions by processing the firing activities of the reservoir. Via its nonlinear dynamics, the reservoir projects the input spike trains into a high-dimensional space of the network transient state, and memorizes the inputs received in the past. In the standard LSM model, only the feed-forward synapses projecting from the reservoir to the readout layer are plastic, which shall be trained properly to ensure good classification performance [3]–[5].

The liquid state machine also provides an appealing paradigm for realizing energy-efficient VLSI learning processors. General-purpose processor architectures may be facilitated by utilizing a shared common reservoir for processing multiple tasks [6]. The inherent resilience of the LSM computational model can be leveraged for error and process variation tolerance in highly-scaled modern CMOS technologies. Recently, VLSI LSM processors and accelerators have been demonstrated [6]–[9].

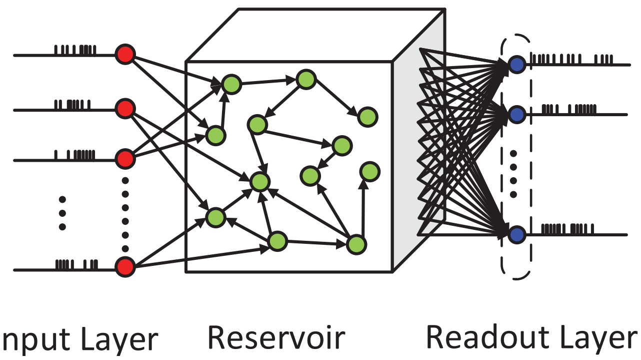

Fig. 1. The model of the liquid state machine.

Training general spiking neural networks is a long-standing challenge. [10] proposes the SpikeProp algorithm that trains feed-forward SNNs by propagating error back in time. While being of a theoretical interest, numerically computing the derivatives of the error function with respect to synaptic weights in terms of spike times is extremely involved. SpikeProp-like algorithms are far from being mature and have yet to be demonstrated for meaningful real-world applications.

To this end, the liquid state machine offers a good tradeoff between training feasibility and computational power. The standard LSM model has a fixed recurrent reservoir and deals with a much simpler training problem: only the feed-forward synapses projecting from the reservoir to the readout layer (referred to as *readout synapses*) need to be trained, which is referred to as *readout training* in this paper. [1]

Instead of using numerical techniques that involve matrix factorizations, the recent work of [5] introduces a biologically-inspired spike-dependent readout training approach with the advantages being local and amenable to VLSI implementation. However, the key limitation of this approach is that good performance is typically guaranteed only with full connectivity between the reservoir and readout, which contributes significantly to the overall network complexity and is also costly from a hardware point of view.

[1]Note that there exist attempts to train a plastic reservoir, cf. [9].

The above challenges motivate us to seek an alterative for readout training. To this end, spike-timing-dependent plasticity (STDP) [11], [12], a well-known unsupervised learning mechanism, is able to locally tune spiking neural networks according to temporal spike correlations and produce interesting self-organizing behaviors. Towards supervised learning which we target in this paper, ideas of combining supervision and STDP have been explored for precisely timed spike reproduction and decision making [13]–[15], however, without demonstrating success for real-world tasks.

For the first time, we target the following objectives under the context of the liquid state machine:

- **Objective-1**: develop supervised STDP mechanisms for readout training with improved learning performance for real-life applications;
- **Objective-2**: develop supervised STDP based techniques for sparsifying readout synapses so as to reduce network complexity and enable efficient hardware realization.

It is important to note that one challenge associated with Objective-1 and Objective-2 is that they are *competing* objectives in the sense that sparsity in readout synapses can easily degrade learning performance. In this paper, both objectives are achieved under a unifying biologically motivated calcium-modulated supervised STDP approach.

Towards the first objective, we propose a new calcium-modulated learning algorithm based on supervised STDP, dubbed $CaL\text{-}S^2TDP$, and demonstrate its improved performance for readout training. One important limitation of the earlier work on supervised STDP is that the issue of synaptic weight saturation has not been addressed. Without a carefully-chosen stop-learning mechanism, continuous ongoing weight modifications may quickly saturate a synaptic weight, overwhelming the synapse by the past experience and preventing it from responding to new stimuli [16]. This can result in bad utilization of memory that is presented in the network and poor learning performance. The problem of weight saturation exacerbates on digital hardware where each synaptic weight is realized using a limited number of bits and tuning range. Furthermore, standard STDP rules conduct continuous weight updates and may trigger many small-valued weight updates, resulting in bad hardware memory access efficiency.

In $CaL\text{-}S^2TDP$, supervision is realized by the combined use of a classification teacher (CT) signal and a new *depressive* STDP rule. For a given input class, the CT promotes the firing activity of targeted the readout neurons by injecting a positive current which serves as the supervision. It also addresses the robustness limitation of standard STDP mechanisms by making it possible to initiate the STDP-based temporal learning process regardless of initial weight values. Motivated by a large variety of STDP mechanisms discovered in the brain [17], we engine the depressive STDP to provide supervision to readout neurons that are desired to have low firing activity for the given input class.

To improve learning performance and address the challenge of weight saturation, we employ probabilistic weight updates and a stop-learning mechanism. Stop learning is trigged by monitoring the calcium concentration of the post-synaptic neuron, which is modeled by low-pass filtering the post-synaptic spike train. Our calcium-modulated supervised STDP approach, for the first time, combines STDP-based temporal learning with modulation provided by the averaged firing level. Using the spoken English letters from the TI46 Speech Corpus [18] as a real-world speech recognition benchmark, we demonstrate that $CaL\text{-}S^2TDP$ significantly improves the recognition rate by up to 25% over a reference supervised STDP rule. Compared to the competitive non-STDP spike-based learning rule in [5], $CaL\text{-}S^2TDP$ improves the recognition rate by up to 2.7%.

Towards the second objective, we propose a new calcium-modulated sparsification algorithm based on supervised STDP, dubbed $CaS\text{-}S^2TDP$, for readout synapse sparsification and demonstrate that it can produce a high-degree of sparsity without significant degradation of learning performance. In the liquid state machine, readout synapses play a significant role in classification decision making. A high-degree of connectivity, often full connectivity, between the reservoir and readout layer must be realized with high-resolution synapses for good learning performance. Consequently, the readout synapses contribute greatly to the overall network complexity, and also to the silicon overhead and energy dissipation of hardware-based LSM processors. To date, the question of how to simultaneously achieve good learning and sparsity in readout synapses remains to be answered.

We achieve the two competing objectives by employing a two-step methodology: sparsificaiton by $CaS\text{-}S^2TDP$ followed by readout training by $CaL\text{-}S^2TDP$. Essentially, $CaS\text{-}S^2TDP$ exploits the automatic competition among afferent synapses of each readout neuron mediated by a typical unsupervised STDP mechanism [19] to produce a bimodal weight distribution with desired sparsity. Under the framework of calcium-modulated supervised STDP, $CaS\text{-}S^2TDP$ adds a teacher signal, called *sparsity teacher*, and a relaxed stop-learning rule, to robustly sparsify the readout synapses while responding to the spatio-temporal structures of the presented training inputs. The sparsity discovered by $CaS\text{-}S^2TDP$ is carried over to the second full-blown training phase based on $CaL\text{-}S^2TDP$. The seamless integration of the two proposed algorithms can prune out up to 30% of readout synapses without causing significant performance degradation.

II. Existing STDP Rules and their limitations

The standard STDP is a local unsupervised Hebbian learning mechanism realizing synaptic plasticity based on the relative firing timing orders of the presynaptic and postsynaptic neurons [11], [12]. The long-term potentiation (LTP) of the synapse w_{ij} occurs if the presynaptic neuron j fires before the postsynaptic neuron i. A presynaptic spike that follows postsynaptic spike produces long-term depression (LTD) of the synapse. The amount of synaptic modification depends on the temporal difference $\Delta t = t_{\text{post}} - t_{\text{pre}}$ between each pair of pre- and postsynaptic spikes:

$$\begin{aligned} \Delta w^{+} &= A_{+}(w) \cdot e^{-\frac{|\Delta t|}{\tau_{+}}} \qquad \text{if } \Delta t > 0 \\ \Delta w^{-} &= A_{-}(w) \cdot e^{-\frac{|\Delta t|}{\tau_{-}}} \qquad \text{if } \Delta t < 0, \end{aligned} \tag{1}$$

where Δw^{+} and Δw^{-} represent the weight change induced by LTP and LTD, $\tau_{\pm}$ are the time constants, and $A_{\pm}(w)$ determine the strength of LTP/LTD, respectively. A typical STDP characteristics is plotted in Fig. 2.

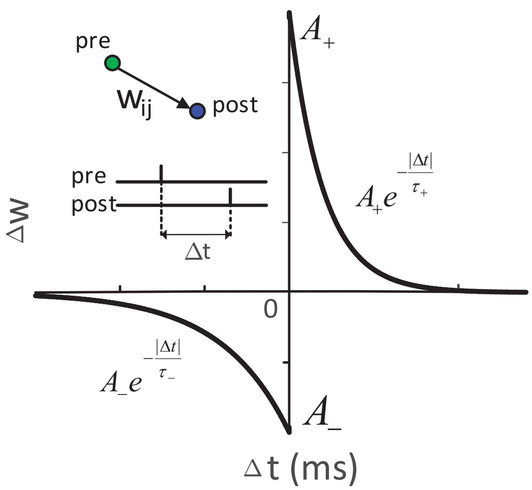

Fig. 2. A typical STDP characteristics.

While the standard unsupervised STDP can be relatively straightforwardly applied to spiking neural networks, the lack of supervision disqualifies it as a choice for readout training. Although supervised STDP mechanisms such as [13]–[15] have been explored, so far no success has been demonstrated towards applying them to real-life applications. As discussed in Section I, these approaches may also suffer from synaptic weight saturation and inefficiency for hardware realization.

III. Proposed Deterministic Supervised STDP without Calcium Modulation

Working towards deriving the proposed $CaL\text{-}S^2TDP$ algorithm, we first present a simpler STDP algorithm, dubbed $D\text{-}S^2TDP$. $D\text{-}S^2TDP$ performs deterministic weight updates, has all essential components of $CaL\text{-}S^2TDP$, but lacks probabilistic weight updates and calcium modulation of $CaL\text{-}S^2TDP$. $D\text{-}S^2TDP$ also serves as a reference of comparison for $CaL\text{-}S^2TDP$ in our experimental study.

A. Mathematical Interpretation for Supervised STDP

As a common practice, let us assume that the classification decision is decoded by choosing the class label of the readout neuron with the highest firing activity (frequency) in the readout layer. Therefore, a supervised training algorithm shall: 1) maximize the firing rate of the readout neuron whose class label corresponds to the presented input sample, referred to as "desired neuron"; and 2) minimize the firing rates of all other readout neurons, referred to as "undesired neurons". We argue that both 1) and 2) can be achieved by solving the following optimization problem:

$$\begin{aligned} \underset{\boldsymbol{f_j^i}}{\text{maximize}} \quad & \sum_{i=1}^{N} \left(f_{c(i)}^{i}(X_i, W) - \sum_{j \neq c(i)}^{C} f_j^i(X_i, W) \right) \\ \text{subject to} \quad & f_j^i \geq 0, \end{aligned} \tag{2}$$

where N is total number of training samples, C is the number of input classes, X_i is the i_{th} input temporal sample, $c(i)$ is the class label for X_i, f_j^i is the firing frequency of the j_{th} readout neuron under the i_{th} input, and W is the vector of all readout synaptic weights. Here, we maximize the difference in summed firing rate between the desired neuron and all undesired neurons so as to minimize the classification error over the N training samples. However, solving (2) in a mathematically exact manner is a formidable task.

B. Proposed $D\text{-}S^2TDP$ Algorithm

Instead, we take a more feasible biologically-inspired approach with respect to (2) as shown in Fig. 3 (a). The proposed $D\text{-}S^2TDP$ algorithm forces the desired neuron to fire at an elevated level via the positive current injected by a classification teacher (CT) signal. Each afferent synapse of the desired neuron is further mediated by a standard STDP rule. To suppress undesired neurons, we employ a novel depressive STDP rule for their afferent synapses.

To see how $D\text{-}S^2TDP$ serves the basic needs of this work, we recall that the standard STDP rule used for afferent synapses of the desired neuron conducts synaptic modification locally and renders the postsynaptic (desired) neuron sensitive to temporal presynaptic firing patterns. Since the causal order (i.e., pre-before-post) of spike pairs leads to synaptic potentiation, the STDP correlates the presynaptic firing events with the modulated postsynaptic firing patterns in a way such that the desired neuron is more likely to fire in presence of presynaptic firing events. As illustrated in Fig. 3(b), when modulated by the CT signal, the desired neuron i_1 emits two spikes after a presynaptic spike, resulting in potentiation of w_{i_1} and making itself more likely to respond to future firings of the presynaptic neuron j. Therefore, we can maximize the firing frequency of the desired neuron by potentiating the synapses that contribute to its firing. The presence of CT also makes the above process robust by initializing STDP-based LTP/LTD even with low initial presynaptic weight values.

We depress plastic synapses that may evoke firing of undesired neurons. As depicted in Fig. 3(c) when the undesired postsynaptic neuron i_2 fires, the pre-before-post spike pattern induces depression to w_{i_2} as determined by the novel depressive STDP rule. As such, we prevent the undesired neurons from learning from training samples of a different input class. Note also that for both desired and undesired neurons, the depression invoked by the anti-causal (i.e., post-before-pre) timing order enables competition among plastic synapses such that a sparse structure can be learned [19].

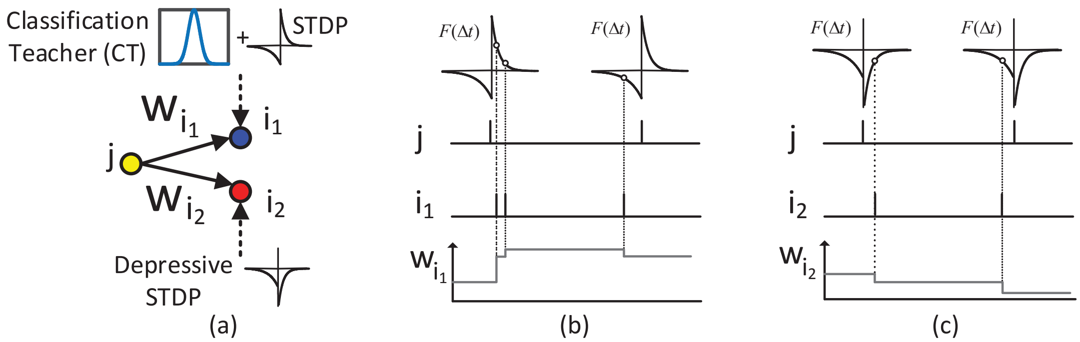

Fig. 3. (a) Proposed D-S^2TDP algorithm. The neuron i_1 is the desired neuron modulated by a classification teacher (CT) and the standard STDP. The neuron i_2 is an undesired one modulated by the depressive STDP for temporal "anti-learning"; (b) and (c) The pre-before-post timing order leads to LTP (LTD) for afferent synapses of the desired (undesired) neuron. The post-before-pre timing order results in depression for both neurons.

IV. Proposed CaL-S^2TDP Training Algorithm

While D-S^2TDP possesses several key ingredients towards effective readout training, we address its limitations, i.e. poor memory retention, synaptic weight saturation and poor weight update efficiency for hardware implementation by extending it to the proposed CaL-S^2TDP algorithm.

Continuous rapid updates of synaptic weights of a limited number of states (e.g. due to a finite synaptic resolution) can result in bad memory retention. This manifests itself in such a way that the most recent experiences are represented and learned by the synapses better than the older ones [20], [21]. We adopt the probabilistic weight update scheme in [22] to slow down the learning process to better utilize network memory capacity. Furthermore, probabilistic updates reduce the committed number of weight updates, leading to improved hardware execution efficiency.

Furthermore, synaptic memory saturation needs to be addressed. Without any stop-learning mechanism, readout synapses are tuned by supervised STDP while continuously extracting temporal information out of the on-going reservoir firing activities. Excessive training can render each readout neuron unresponsive to new stimuli once most of its afferent synapses are over-potentiated or over-depressed, i.e., the synaptic weights are driven to the maximum/minimum value.

A. Postsynaptic Calcium Concentration

Ideally, we may deactivate potentiation of a synapse when its postsynaptic neuron is very active, which suggests that this synapse has been already over-potentiated. Similarly, we shall deactivate synaptic depression when the postsynaptic neuron becomes very inactive. Inspired by [16], we make use of the internal calcium concentration of a postsynaptic neuron as an indicator of its averaged firing level induced by new and old inputs over a long timescale. The calcium concentration $c(t)$ is a function of the postsynaptic neuron activity and modeled using a first-order dynamics:

$$\frac{dc(t)}{dt} = -\frac{c(t)}{\tau_c} + \sum_i \delta(t - t_i), \tag{3}$$

where τ_c is the time constant and the summation is over all postsynaptic spikes arriving at time t_i.

B. Stop-learning for Desired Neuron

We now discuss how to implement a stop-learning mechanism for the desired neuron. First, a threshold c_θ of calcium variable is defined to distinguish active neurons from inactive ones. We then introduce a margin δ and allow potentiation when $c < c_\theta + \delta$. Analogously, depression is allowed when $c > c_\theta - \delta$. Following the principle of Hebbian learning, we further impose a lower bound of c for activating potentiation and an upper bound of c for activating depression. Combining the stop-learning mechanism and probabilistic weight updates gives the CaL-S^2TDP algorithm:

$$\begin{aligned} &w \leftarrow w + \Delta W \ \textit{w/ prob.} \propto |\Delta w^+| \ \text{ if } \Delta t > 0 \ \&\& \\ &\qquad\qquad\qquad\qquad\qquad\qquad c_\theta < c < c_\theta + \delta \\ &w \leftarrow w - \Delta W \ \textit{w/ prob.} \propto |\Delta w^-| \ \text{ if } \Delta t < 0 \ \&\& \\ &\qquad\qquad\qquad\qquad\qquad\qquad c_\theta > c > c_\theta - \delta, \end{aligned} \tag{4}$$

where Δw^+/Δw^- are the weight changes computed based on the employed the STDP rule, and determine the probabilities for committing a fixed weight update of $\pm\Delta W$ for LTP and LTD, respectively. As in Fig. 4(b), a synapse can be potentiated when the calcium concentration c of the desired neuron falls into [c_θ,$c_\theta + \delta$] and depressed when c is in [$c_\theta - \delta, c_\theta$].

C. Stop-learning for Undesired Neurons

Since the depressive STDP is employed for the afferent synapses of undesired neurons, only the second equation in (4) is activated. The CaL-S^2TDP algorithm is further illustrated in Fig. 4(c) and (d) where no long-term modification is induced if the calcium level is too low or too high, different from D-S^2TDP as shown in Fig. 3(b) and (c).

V. Proposed CaS-S^2TDP Sparsification Algorithm

The plastic readout synapses in an LSM often need to be very dense, e.g. forming a full-connectivity between the reservoir and readout, and have high resolution to guarantee good learning performance. This leads to two potential problems:

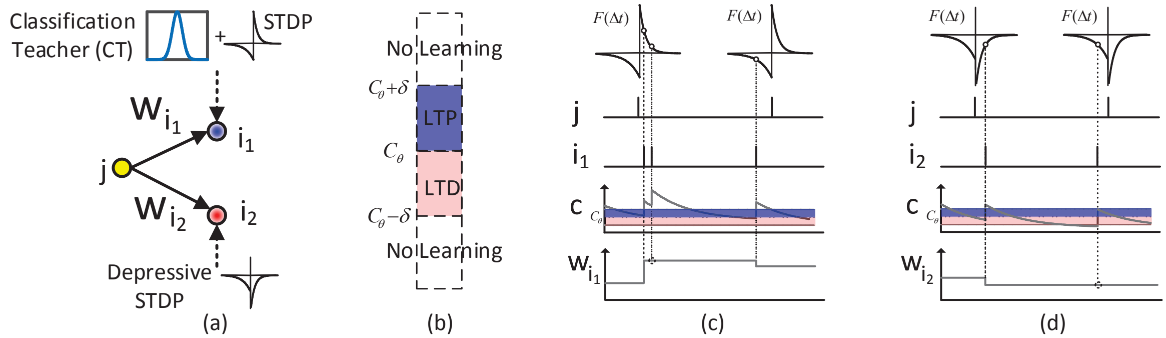

Fig. 4. (a) Proposed $CaL\text{-}S^2TDP$ training algorithm with probabilistic weight updates. The desired neuron i_1 is expected to be active because of CT and the unwanted neuron i_2 is inactive due to the depressive STDP; (b) Stop-learning mechanisms; (c) and (d) The training of desired and undesired synapses. Different from Fig. 3(b) and (c), the LTP or LTD takes place only when the postsynaptic calcium level c falls into the specified range.

over-fitting due to high model complexity, and large overhead for hardware implementation. On the other hand, randomly pruning readout connections can easily degrade performance significantly.

A. Readout Synapse Sparsification

The starting point for the proposed $CaS\text{-}S^2TDP$ sparsification algorithm is the recognition of the fact that different from supervised classification for which neurons are instructed to learn certain firing patterns, the objective of sparsification is to allow sufficient competition among plastic readout synapses. We further recognize that synapses mediated by standard STDP characteristics compete for control of the timing of postsynaptic action potentials. As a result, some synapses to a postsynaptic neuron are strengthened while others are weakened [19]. When properly explored, the above process can lead to a bimodal weight distribution out of which many zero-valued or small-valued synapses can be pruned out. As a common practice, only excitatory plastic synapses are sparsified.

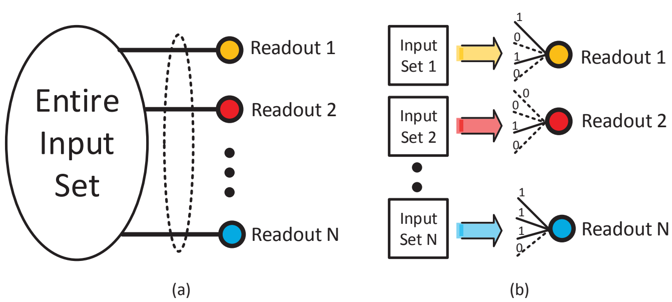

Fig. 5. (a) The non-optimal sparsification based on the entire input set; (b) Optimized sparsification with the corresponding subset of inputs for each readout neuron.

In order to make use of the above ideas for real-life multi-class classification tasks, we make additional important observations. To guarantee good performance, sparsification shall be not be performed blindly, instead, it must take into the spatio-temporal structures embedded in the training samples such that the discovered sparse patterns fit well with the data, and hence do not lead to significant performance loss. This suggests to enable a standard STDP for introducing competitions among the afferent synapses of each readout neuron over the entire training data set, as shown in Fig. 5(a). However, a closer examination reveals that since each readout neuron is associated with a specific class label, it is not necessary to instruct each readout neuron to learn the sparse structure of the entire input data. A more optimal approach is to constrain the finding of sparsity within of the subset of training data of the corresponding input class for each readout neuron as shown in Fig. 5(b). This leads to the maximum sparsity.

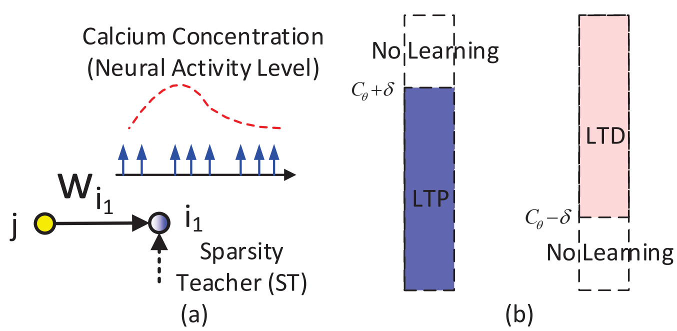

Fig. 6. (a) The $CaS\text{-}S^2TDP$ sparsification algorithm. The activity level of the selected readout neuron i_1 is boosted by the sparsity teacher (ST). (b) stop learning for readout synapse sparsification.

Akin to the $CaL\text{-}S^2TDP$ training algorithm, we make readout sparsification robust by introducing an external sparsity teacher (ST) (Fig. 6(a)), whose job is to reliably bring up the firing activity of each readout neuron to start synaptic competition modulated by the STDP. To maintain good learning performance, we also introduce a stop-learning mechanism. As shown in Fig. 6(b), this stop-learning mechanism is more relaxed with a wider calcium range for both LTP and LTD to avoid undesirable bias in calcium regulation and maximize sparsity. The resulting $CaS\text{-}S^2TDP$ sparsification algorithm is summarized as:

$$\begin{aligned} w \leftarrow w + \Delta W \ \textit{w/ prob.} \propto |\Delta w^{+}| \ \text{if } \Delta t > 0 \ \&\& \\ c < c_{\theta} + \delta \\ w \leftarrow w - \Delta W \ \textit{w/ prob.} \propto |\Delta w^{-}| \ \text{if } \Delta t < 0 \ \&\& \\ c_{\theta} - \delta < c. \end{aligned} \tag{5}$$

VI. Combined Sparsification and Training

The integration of the proposed sparsification and classification algorithms is summarized in Fig. 7. First, CaS-S^2TDP is applied to sparsify readout synapses. After removing the synapses of a zero-valued weight, the remaining synaptic weights are used as a starting point for training of the readout based on CaL-S^2TDP.

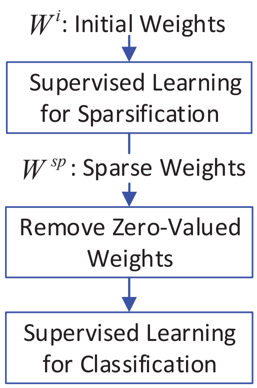

Fig. 7. Two-step sparsification and classification.

Because of the self-organizing behavior introduced by the STDP, the proposed CaS-S^2TDP sparsification algorithm learns to capture the spatio-temporal structures of the input spikes. Therefore, unlike blind synapse pruning, the proposed approach makes it possible to pass the discovered sparsity from the sparsification stage to the training phase, and produce good learning performance in the end.

VII. Experimental Settings and Benchmark

Using the approach described in [5], two LSMs with 135 and 90 reservoir neurons are set up on a 3D grid, respectively. 80% of the reservoir neurons are excitatory while the rest of them are inhibitory. Since the adopted benchmark is spoken English letter recognition, there are 26 neurons in the readout layer, which is fully connected to the reservoir through plastic synapses. Furthermore, we adopt the discrete LIF neuronal model and the second-order synaptic model described in [5].

The parameters of the STDP algorithms described in this work are selected by exploring the design space to a certain degree and we summarize the chosen ones in Table I. The maximum readout synaptic weight $W_{\max}$ is set to 8.0. The initial weights of excitatory readout plastic synapses are set to 1.0 while inhibitory synaptic weights are initialized to be a random value between 0 and -$W_{\max}$. We set the bit-width of readout synaptic weights to 10 bits.

TABLE I
Parameter settings of the proposed STDP algorithms.

Parameter	Value
A_+	3.0
A_-	1.5
τ_+	4.0
τ_-	8.0
ΔW	0.016
c_θ	5.0
δ	2.0
τ_c	64.0

The adopted benchmark is a subset of the TI46 speech corpus [18], which contains 10 utterances of each English letter from “A” to “Z”. The speech samples were recorded from a single speaker. 260 samples are in this benchmark. The time domain speech signals are preprocessed by Lyon’s passive ear model [23], and encoded into 78 spike trains using the BSA algorithm [24]. Each input spike train generated in the preprocessing stage is sent to 32 randomly selected reservoir neurons with a fixed weight randomly chosen to be 2 or -2.

During the supervised readout sparsification phase, all speech samples are presented to the reservoir one by one while the CaS-S^2TDP algorithm is only applied to tune the plastic synapses of the corresponding readout neuron while other readout neurons are isolated. The process is repeated for a sufficient number of iterations until the distribution of the readout synaptic weights reaches to the steady-state. Then, we permanently remove zero-valued plastic weights and train the readout layer with the proposed CaL-S^2TDP algorithm for final training. A 5-fold cross validation scheme is adopted to test the recognition performance for each LSM by randomly dividing entire speech samples into 5 groups. The recognition decision is made right after each testing speech sample is presented. At this time, the class label of the readout neuron with the highest firing rate is regarded as the classification decision. The readout layer is trained for 500 iterations in order to get decent learning performance.

VIII. Experimental Results

Using the experimental setups described in Section VII, we compare the learning performance of CaL-S^2TDP to both the simpler D-S^2TDP algorithm of Section III and the competitive non-STDP spike-dependent algorithm of [5]. We also compare the proposed CaS-S^2TDP based sparsification algorithm with random and variance-based pruning [9] for both of which the algorithm of [5] is used to train the readout.

A. Classification Performance of CaL-S^2TDP

We use the adopted benchmark described in Section VII to test the LSM recognition rates with three different readout learning algorithms and the results are shown in Table II. The standard deviations are obtained from five experiments. Here, the proposed readout sparsification is not performed before the application of CaL-S^2TDP. It turns out that D-S^2TDP produces very low recognition rates under both reservoir sizes, indicating that $D\text{-}S^2TDP$ is ineffective for the readout learning when the synapses have a finite resolution. In Fig. 8, we visualize the distribution of the readout plastic weights obtained after running the first ten training iterations. For $D\text{-}S^2TDP$, a considerable number of plastic readout weights quickly reach to the highest or lowest weight value, which is a direct sign of synaptic memory saturation. Fig. 8(a) and (c) also suggest that the poor performance of $D\text{-}S^2TDP$ may be attributed to the occurrence of synaptic weight saturation, resulting from the lack of stop-learning mechanisms.

TABLE II
RECOGNITION RATES OF THE LSMS WITH DIFFERENT READOUT TRAINING ALGORITHMS.

Reservoir Size	**[5]**	$D\text{-}S^2TDP$	$CaL\text{-}S^2TDP$
135	$92.3 \pm 0.4\%$	$68.8 \pm 0.1\%$	**93.8** $\pm 0.5\%$
90	$89.6 \pm 0.5\%$	$67.3 \pm 0.4\%$	**92.3** $\pm 0.4\%$

The proposed $CaL\text{-}S^2TDP$ algorithms achieves good learning performances of 93.8% with 135 reservoir neurons and 92.3% with 90 reservoir neurons, respectively. Equipped with the probabilistic update and stop learning conditions, $CaL\text{-}S^2TDP$ significantly outperforms the simpler $D\text{-}S^2TDP$ by 25% in terms of recognition rate for both reservoir sizes. The dominance of the proposed $CaL\text{-}S^2TDP$ algorithm can be further explained by the weight distribution in Fig. 8 (b) and (d), where less plastic weights are saturated compared to the simpler algorithm.

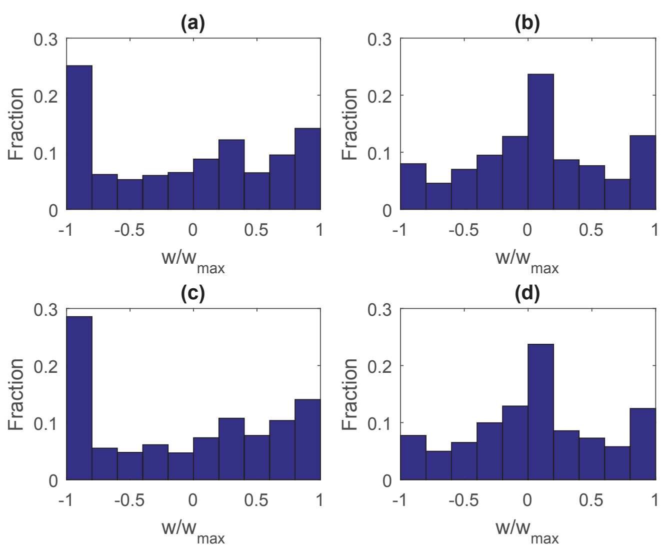

Fig. 8. The distribution of readout synaptic weights after running first few training iterations. (a) and (c): the distribution obtained under $D\text{-}S^2TDP$ with 90 and 135 neurons in the reservoir, respectively; (b) and (d): the distribution under $CaL\text{-}S^2TDP$ with the same two reservoir sizes.

To the best knowledge of the authors, the best reported performance on the same benchmark achieved by the standard LSM with 135 reservoir neurons is 92.3% [5]. In comparison to this algorithm, the proposed supervised STDP algorithm $CaL\text{-}S^2TDP$ outperforms it by 1.5% with the reservoir size of 135 neurons. $CaL\text{-}S^2TDP$ also produces a good recognition rate of 92.3% when the size of the reservoir is reduced to 90 neurons, achieving a performance boost of 2.7% in this case.

B. Sparsity Obtained by $CaS\text{-}S^2TDP$.

We examine the sparsity of the readout due to the proposed $CaS\text{-}S^2TDP$ based sparsification scheme. After training the readout based on the proposed two-step sparsification and classification, we report the percentages of zero-valued readout synapses and the final learning performances in Table III. We implement the random pruning policy and variance-based pruning of [9] and train the readout with the bio-inspired algorithm [5] for comparison. The obtained sparsity as well as learning performances are also shown in Table III. Using the random pruning policy as a baseline, we plot the performance boosts achieved by the variance-based and the proposed approach in Fig. 9.

TABLE III
RECOGNITION PERFORMANCES WITH THREE SPARSIFICATION METHODS.

	Recognition Performance		
Sparsity	135 Reservoir Neurons		
%	Random	Variance	Proposed
10%	$90.7 \pm 0.6\%$	$91.5 \pm 0.4\%$	$92.7 \pm 0.5\%$
18%	$90.4 \pm 0.5\%$	$90.4 \pm 0.8\%$	$91.9 \pm 0.4\%$
30%	$83.8 \pm 1.0\%$	$85.0 \pm 1.3\%$	$90.7 \pm 0.4\%$
Sparsity	90 Reservoir Neurons		
%	Random	Variance	Proposed
10%	$86.9 \pm 1.0\%$	$87.7 \pm 0.7\%$	$91.5 \pm 0.4\%$
18%	$85.7 \pm 1.2\%$	$86.9 \pm 0.8\%$	$90.7 \pm 0.4\%$
30%	$89.2 \pm 0.8\%$	$89.6 \pm 0.8\%$	$91.1 \pm 0.4\%$

As shown in Table III, randomly removing the readout synapses can lead to apparent performance degradation. The variance-based policy performs lightly better than the random baseline but the improvement is not significant. In comparison to the above two approaches, the proposed $CaS\text{-}S^2TDP$ algorithm delivers a decent learning performance under all considered levels of sparsity for different reservoir sizes as shown in Table III. Importantly, the proposed approach substantially improves the effectiveness of readout sparsification compared to the random baseline. As shown in Fig. 9, the STDP-based approach is superior than the variance-based rule. The proposed approach can boost the random baseline performance up to 6.9% whereas the maximum boost for variance-based approach is only 1.2%.

IX. CONCLUSIONS

In this paper, we have proposed a novel calcium-modulated supervised STDP approach for both classification and sparsification, targeting efficient readout training in the context of the liquid state machine. Via a classification teacher signal, the proposed depressive STDP and probabilistic weight updates,

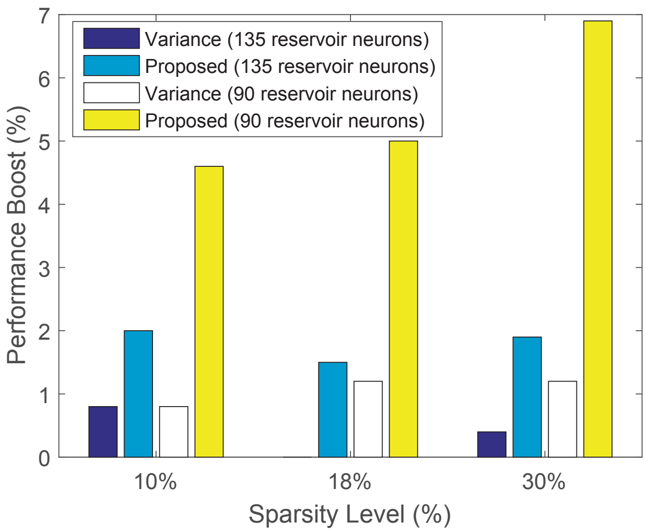

Fig. 9. The performance boosts over the random pruning policy achieved by two different readout sparsification approaches. The proposed $CaS\text{-}S^2TDP$ algorithm significantly boosts performance compared to the random baseline and outperforms the variance-based approach.

$CaL\text{-}S^2TDP$ robustly delivers good learning performance with finite weight resolutions. $CaL\text{-}S^2TDP$ addresses the issue of synaptic memory saturation by imposing an stop learning condition modulated by the postsynaptic calcium concentration. Sparse readout layers can be obtained by the presented $CaS\text{-}S^2TDP$ readout sparsification approach with little performance gradation. Using speech recognition as a realistic benchmark, we have shown that $CaL\text{-}S^2TDP$ outperforms all other studied bio-plausible supervised training algorithms and $CaS\text{-}S^2TDP$ based readout sparsification mechanism is superior over all other investigated approaches.

ACKNOWLEDGMENT

This material is based upon work supported by the National Science Foundation under Grant No. CCF-1639995 and the Semiconductor Research Corporation (SRC) under Task 2692.001. The authors would like to thank High Performance Research Computing (HPRC) at Texas A&M University for providing computing support.

REFERENCES

[1] M. Lukoševičius and H. Jaeger, "Reservoir computing approaches to recurrent neural network training," *Computer Science Review*, vol. 3, no. 3, pp. 127–149, 2009.

[2] W. Maass, T. Natschläger, and H. Markram, "Real-time computing without stable states: A new framework for neural computation based on perturbations," *Neural computation*, vol. 14, no. 11, pp. 2531–2560, 2002.

[3] D. Verstraeten, B. Schrauwen, D. Stroobandt, and J. Van Campenhout, "Isolated word recognition with the liquid state machine: a case study," *Information Processing Letters*, vol. 95, no. 6, pp. 521–528, 2005.

[4] A. Ghani, T. M. McGinnity, L. P. Maguire, and J. Harkin, "Neuro-inspired speech recognition with recurrent spiking neurons," in *Artificial Neural Networks-ICANN 2008*. Springer, 2008, pp. 513–522.

[5] Y. Zhang, P. Li, Y. Jin, and Y. Choe, "A digital liquid state machine with biologically inspired learning and its application to speech recognition," *IEEE Transactions on Neural Networks and Learning Systems*, vol. 26, no. 11, pp. 2635–2649, Nov. 2015.

[6] Q. Wang, Y. Jin, and P. Li, "General-purpose LSM learning processor architecture and theoretically guided design space exploration," in *Biomedical Circuits and Systems Conference (BioCAS), 2015 IEEE*. IEEE, 2015, pp. 1–4.

[7] S. Roy, A. Banerjee, and A. Basu, "Liquid state machine with dendritically enhanced readout for low-power, neuromorphic VLSI implementations," *Biomedical Circuits and Systems, IEEE Transactions on*, vol. 8, no. 5, pp. 681–695, 2014.

[8] Q. Wang, Y. Li, and P. Li, "Liquid state machine based pattern recognition on fpga with firing-activity dependent power gating and approximate computing," in *2016 IEEE International Symposium on Circuits and Systems (ISCAS)*, May 2016, pp. 361–364.

[9] Y. Jin, Y. Liu, and P. Li, "SSO-LSM: A sparse and self-organizing architecture for liquid state machine based neural processors," in *2016 IEEE/ACM International Symposium on Nanoscale Architectures (NANOARCH)*, July 2016, pp. 55–60.

[10] S. M. Bohte, J. N. Kok, and H. La Poutre, "Error-backpropagation in temporally encoded networks of spiking neurons," *Neurocomputing*, vol. 48, no. 1, pp. 17–37, 2002.

[11] G.-q. Bi and M.-m. Poo, "Synaptic modification by correlated activity: Hebb's postulate revisited," *Annual review of neuroscience*, vol. 24, no. 1, pp. 139–166, 2001.

[12] A. Morrison, M. Diesmann, and W. Gerstner, "Phenomenological models of synaptic plasticity based on spike timing," *Biological cybernetics*, vol. 98, no. 6, pp. 459–478, 2008.

[13] F. Ponulak and A. Kasinski, "Supervised learning in spiking neural networks with ReSuMe: sequence learning, classification, and spike shifting," *Neural Computation*, vol. 22, no. 2, pp. 467–510, 2010.

[14] J.-P. Pfister, T. Toyoizumi, D. Barber, and W. Gerstner, "Optimal spike-timing-dependent plasticity for precise action potential firing in supervised learning," *Neural computation*, vol. 18, no. 6, pp. 1318–1348, 2006.

[15] J.-M. P. Franosch, S. Urban, and J. L. van Hemmen, "Supervised spike-timing-dependent plasticity: A spatiotemporal neuronal learning rule for function approximation and decisions," *Neural computation*, vol. 25, no. 12, pp. 3113–3130, 2013.

[16] J. M. Brader, W. Senn, and S. Fusi, "Learning real-world stimuli in a neural network with spike-driven synaptic dynamics," *Neural computation*, vol. 19, no. 11, pp. 2881–2912, 2007.

[17] N. Caporale and Y. Dan, "Spike Timing-Dependent Plasticity: a hebbian learning rule," *Annu. Rev. Neurosci.*, vol. 31, pp. 25–46, 2008.

[18] "The TI46 Speech Corpus," http://catalog.ldc.upenn.edu/LDC93S9.

[19] S. Song, K. D. Miller, and L. F. Abbott, "Competitive hebbian learning through spike-timing-dependent synaptic plasticity," *Nature neuroscience*, vol. 3, no. 9, pp. 919–926, 2000.

[20] D. J. Amit and S. Fusi, "Constraints on learning in dynamic synapses," *Network: Computation in Neural Systems*, vol. 3, no. 4, pp. 443–464, 1992.

[21] D. J. Amit and S. Fusi, "Learning in neural networks with material synapses," *Neural Computation*, vol. 6, no. 5, pp. 957–982, 1994.

[22] Y. Jin and P. Li, "AP-STDP: A novel self-organizing mechanism for efficient reservoir computing," in *International Joint Conference on Neural Networks (IJCNN)*, July 2016, pp. 1158–1165.

[23] R. F. Lyon, "A computational model of filtering, detection, and compression in the cochlea," in *Acoustics, Speech, and Signal Processing, IEEE International Conference on ICASSP'82.*, vol. 7. IEEE, 1982, pp. 1282–1285.

[24] B. Schrauwen and J. Van Campenhout, "BSA, a fast and accurate spike train encoding scheme," in *International Joint Conference on Neural Networks (IJCNN)*, vol. 4. IEEE Piscataway, NJ, 2003, pp. 2825–2830.